ISA Transactions ■ (■■■■) ■■■–■■■

Contents lists available at ScienceDirect

ISA Transactions

journal homepage: www.elsevier.com/locate/isatrans

Control of discrete time systems based on recurrent Super-Twisting-like algorithm

I. Salgado [a], S. Kamal [e], B. Bandyopadhyay [b], I. Chairez [c,*], L. Fridman [d]

[a] Centro de Innovación y Desarrollo Tecnológico en Cómputo (CIDETEC), Instituto Politécnico Nacional, Mexico City, Mexico
[b] SYSCON, Indian Institute of Technology, Bombay, Mumbai, India
[c] Departamento de Bioprocesos, Unidad Profesional Interdisciplinaria de Biotecnología (UPIBI), Instituto Politécnico Nacional, Av. Acueducto de Guadalupe s/n col. Barrio la Laguna, Gustavo A. Madero, Mexico City, DF, Mexico
[d] Engineering Universidad Nacional Autónoma de México, Mexico City, Mexico
[e] Department of Systems Innovation and Informatics, Kyushu Institute of Technology, Kitakyushu, Japan

ARTICLE INFO

Article history:
Received 14 September 2015
Received in revised form
8 February 2016
Accepted 23 April 2016
This paper was recommended for publication by Oscar Camacho

Keywords:
Sliding mode control
Discrete-time super twisting algorithm
Sliding mode differentiator
Electro-mechanical systems

ABSTRACT

Most of the research in sliding mode theory has been carried out to in continuous time to solve the estimation and control problems. However, in discrete time, the results in high order sliding modes have been less developed. In this paper, a discrete time super-twisting-like algorithm (DSTA) was proposed to solve the problems of control and state estimation. The stability proof was developed in terms of the discrete time Lyapunov approach and the linear matrix inequalities theory. The system states trajectories were ultimately bounded inside a small region dependent on the sampling period. Simulation results tested the DSTA. The DSTA was applied as a controller in a Furuta pendulum and as a signal differentiator and as a controller in close loop for a DC motor.

1. Introduction

Advanced control techniques such as Sliding Modes (SM) allow the control of uncertain nonlinear systems when they are affected by modeling imprecisions or external perturbations. Classical features exhibited by sliding modes are robustness with respect to external matched uncertainties and finite time convergence. A SM scheme is obtained by inducing a discontinuity in the control structure. The discontinuous injection must be designed such that the trajectories of the system are forced to remain on some surface defined in the state space. The resulting motion on that surface is referred as sliding mode [1]. In continuous time systems, the SM have been extensively studied, the main theoretical results are presented in [1,2], and references therein. In continuous time, the second order sliding mode solutions (SOSM) preserve the main characteristics of classical SM while reduce the undesirable chattering effect [3,4].

On the other hand, SM in discrete-time or discrete sliding modes (DSM) generate the so-called quasi-sliding regime (QSM) and it has been less developed than the continuous case. The first ideas in DSM were introduced by [5,6] where a QSM is established for systems with relative degree one. In [7], the study of SISO nonlinear systems with relative degree more than one is treated. A new definition of a QSM regime is addressed in [8], where the motion of the system is restricted inside a certain band around the sliding hyperplane. In [9,10], some new developments on QSM have been reported for several classes of discrete-time linear systems. An approach to control discrete time systems using the fast output technique is considered when the system states are not needed on-line [11]. The idea of second order sliding mode control in discrete time systems has been introduced in terms of certain class of discretizations [12]. Although in [13,14] a sort of discretization has been applied on high order sliding mode controllers, the results are not reported in the literature so far, which deals with the concept of high-order discrete time sliding mode control (HDSM).

In this study, a new strategy to develop a Lyapunov like function for the so-called discrete time Super-Twisting-like Algorithm (DSTA) is proposed. This name is used considering the similarities between the Euler discretization applied on the continuous version of the super-twisting method. In this scheme, the system trajectories are confined into a boundary layer in the vicinity of the sliding surface and stays inside it forever. The upper bound for the tracking error applying the DSTA is depending on the sampling period to the square power. The stability analysis is made in terms

* Corresponding author.
E-mail address: jchairezo@ipn.mx (I. Chairez).

http://dx.doi.org/10.1016/j.isatra.2016.04.024
0019-0578/

of the discrete-time Lyapunov theory. Sufficient conditions for the existence of QSM by means of a LMI are proposed.

In Section 2, the concept of high-order sliding modes (HOSM) is introduced. Some mathematical background on the stability of discrete time nonlinear systems is given in Section 3. Then, a discrete time super-twisting control, a particular type of discrete time second order sliding mode control is presented in Section 4. The result about the convergence of the proposed algorithm is established in terms of a simple quadratic Lyapunov function. In Section 5, numerical examples are presented. The first example is regarding the stabilization problem of a Furuta Pendulum. Then, the DSTA is tested as a robust signal differentiator following the result given in [15]. In close loop, the trajectory tracking problem for a DC motor is presented as a second example. Finally in Section 6 some conclusions are established.

2. Concept of high-order sliding modes

First, let us briefly introduce the high-order SM controllers concept applied on continuous time systems. Consider a smooth dynamic system $\dot{x}=f(x)+g(x)u$, where $x\in\mathbb{R}^n$ is the system state, $u\in\mathbb{R}$ is the scalar control, $f:\mathbb{R}^n\to\mathbb{R}^n$ and $g(x):\mathbb{R}^n\to\mathbb{R}^n$ are some smooth functions. High-order sliding manifold is given as follows. Consider that the set

$$s_r=\left\{x:\frac{d^k}{dt^k}\sigma(x)=0,\quad k=0,1,\ldots,r-1\right\},\tag{1}$$

is non-empty and consists locally of Filippov trajectories, where σ is a smooth function (this is considered as the sliding variable). The trajectories of these functions provide the successive time derivative of σ. The motion on set (1) is called rth-order sliding mode [18], which gives the dynamic smoothness degree in some vicinity of the sliding mode.

The relative degree r of the system is assumed to be constant and known. In other words, the first time at control explicitly appears in the rth total time derivative of σ is $\sigma^r=h(t,x)+l(t,x)u$, where

$$h(t,x)=\sigma^r|_{u=0},$$
$$l(t,x)=\frac{\partial}{\partial u}\sigma^r\neq 0,\quad 0<k_m\le\frac{\partial}{\partial u}\sigma^r\le k_M,$$
$$|\sigma^r|_{u=0}\le c,\quad k_m,k_M,c\in\mathbb{R}^+.$$

For finite time stabilization at origin, u takes the form given by $u=\varphi(\sigma,\dot{\sigma},\ldots,\sigma^r)$. Based on this concept, several sliding mode controllers (the sub-optimal controller [16], twisting controller [17], the terminal sliding mode controller [18] and super twisting controller [19]) were proposed in continuous time. Moreover, a general output based controller for rth relative degree system has been also developed.

Formulating HDSM, Wang et al., firstly discretized the continuous time SMC and after that equivalent control based SMC system with the relative degree higher than one is formulated in the canonical form for designing the controller [13]. To define the sliding set, they replaced high order derivatives of the sliding mode by their respective discrete counterpart such as $\dot{\sigma}(\cdot):=\sigma(k+1)$. Using invertible state transformation matrix, they conclude that the original state is asymptotically stable.

3. Mathematical background

The following result is needed to demonstrate the convergence results for the DSTA.

Theorem 1. *[20] Consider the nonlinear dynamic system*

$$x_1(k+1)=f_1(x_1(k),x_2(k)),\quad x_1(0)=x_{10}$$
$$x_2(k+1)=f_2(x_1(k),x_2(k)),\quad x_2(0)=x_{20}\tag{2}$$

where $x_1\in D\subseteq\mathbb{R}^{n_1}$, $x_2\in\mathbb{R}^{n_2}$, $n_1+n_2=n$, $f_1:\mathbb{R}^n\to\mathbb{R}^{n_1}$ and $f_2:\mathbb{R}^n\to\mathbb{R}^{n_2}$ are continuous smooth functions. Assume that there exists a continuous function $V:D\times\mathbb{R}^{n_2}\to\mathbb{R}$ and a class of $\mathcal{K}$ functions $\alpha(\cdot)$, $\beta(\cdot)$ such that the following inequality is valid

$$\alpha(\|x_1\|)\le V(x_1,x_2)\le\beta(\|x_1\|)$$
$$x_1\in D,\quad x_2\in\mathbb{R}^{n_2}\tag{3}$$

Furthermore, assume that there exists a continuous function $W:D\to\mathbb{R}$ such that $W(x_1)>0$, $\|x_1\|>\mu$,

$$\Delta V(x_1,x_2)\le -W(x_1)$$
$$x_1\in D,\quad x_2\in\mathbb{R}^{n_2}$$

where $\mu>0$, is such that $B_{\alpha^{-1}(\beta(\mu))}(0)\subset D$, where $B_{\alpha^{-1}}$ is a subset of D centered at the origin with radius α^{-1}. Finally, assume that

$$\sup_{(x_1,x_2)\in\overline{B}_\mu(0)\times\mathbb{R}^{n_2}} V(f(x_1,x_2))$$

exists. Then the nonlinear dynamic system (2) is ultimately bounded with respect to x_1, uniformly in x_2 with bound $\varepsilon\triangleq\alpha^{-1}(\eta)$, where

$$\eta>\max\left\{\beta(\mu),\ \sup_{(x_1,x_2)\in\overline{B}_\mu(0)\times\mathbb{R}^{n_2}} V(f(x_1,x_2))\right\}$$

Furthermore, $\limsup_{k\to\infty}\|x_1(k)\|\le\alpha^{-1}(\eta)$. If, in addition $D=\mathbb{R}^n$ and $\alpha(\cdot)$ is a K_∞ class function, then the nonlinear dynamic system (2) is globally ultimately bounded with respect to x_1 uniformly in x_2 with bound ε.

In the previous theorem, the following definition was used.

Definition 1. [20] The nonlinear discrete time dynamic system (2) is uniformly ultimately bounded with bound ε if there exists $\phi>0$ such that, for every $\delta\in(0,\phi)$, exists $T_f=T_f(\delta,\varepsilon)>0$ such that $\|x_0\|<\delta$ implies $\|x(k)\|<\varepsilon$, $k\ge k_0+T_f$. The nonlinear discrete time dynamic system (3) is globally uniformly ultimately bounded with bound ε if for every $\delta\in(0,\infty)$, there is a $T_f=T_f(\delta,\varepsilon)>0$ such that $\|x_0\|<\delta$ implies $\|x(k)\|<\varepsilon$, $k\ge k_0+T_f$.

Remark 1. This definition has the same meaning that finite time convergence in continuous time for discrete time in quasi-sliding mode regimen.

Based on the previous theorem, the next corollary represents the main tool to demonstrate the convergence of the algorithm introduced in this paper.

Corollary 1. [20] *Consider the nonlinear dynamic system (2). Assume that there exist a continuous function $V:D\times\mathbb{R}^{n_2}\to\mathbb{R}$ and a class of $\mathcal{K}$ functions $\alpha(\cdot)$, $\beta(\cdot)$ such that Eq. (3) holds. Furthermore, assume that there exists a $\mathcal{K}$ class function $\gamma:D\to\mathbb{R}$ such that*

$$\Delta V(x_1,x_2)\le-\gamma(\|x_1\|)+\gamma(\mu),$$
$$x_1\in D,\quad x_2\in\mathbb{R}^{n_2}\tag{4}$$

where $\mu>0$ is such that $B_{\alpha^{-1}(\beta(\mu))}(0)\subset D$. Then the nonlinear dynamic system (2) is ultimately bounded with respect to x_1 uniformly in x_2 with bound $\varepsilon\triangleq\alpha^{-1}(\eta)$ where $\eta=\beta(\mu)+\gamma(\mu)$. Furthermore, $\limsup_{k\to\infty}\|x_1\|\le\alpha^{-1}(\eta)$. If, in addition, $D=\mathbb{R}^n$ and $\alpha(\cdot)$ is a class of $\mathcal{K}_\infty$ function, then, the nonlinear dynamic system (2) is globally ultimately bounded with respect to x_1 uniformly in x_2 with bound ε.

These two results are used to develop the stability proof for the DSTA.

Please cite this article as: Salgado I, et al. Control of discrete time systems based on recurrent Super-Twisting-like algorithm. ISA Transactions (2016), http://dx.doi.org/10.1016/j.isatra.2016.04.024

4. Problem statement and main contribution

Consider an uncertain discrete time nonlinear system

$$x(k+1) = (I_{n\times n} + \tau A)x(k) + \tau B u(k) + \tau f(x(k)) \tag{5}$$

where $x \in \mathbb{R}^n$ is the state vector, $u \in \mathbb{R}^m$ is the control input, A, B are constant matrices of appropriate dimensions, and f is an uncertainty/disturbance in the system, τ is the sampling period of the system. The form presented in (5) is usually known as the Euler type discretization of a nonlinear system.

Assume that the following conditions hold

(A1) *rank* $B = m$
(A2) the pair (A, B) is controllable
(A3) the function f is continuous.

It is well-known that under assumptions A1 and A2 there exist a matrix T such that the transformation

$$\begin{bmatrix}\eta\\ \xi\end{bmatrix} = Tx, \quad T = \begin{bmatrix}B^{\perp}\\ B^{+}\end{bmatrix}, \quad B^{+} = (B^{\top}B)^{-1}B^{\top}, \quad B^{\perp}B = 0$$

converts the system (5) in its equivalent regular form given by

$$\begin{aligned}\eta(k+1) &= \eta(k) + \tau A_{11}\eta(k) + \tau A_{12}\xi(k)\\ \xi(k+1) &= \xi(k) + \tau A_{21}\eta(k) + \tau A_{22}\xi(k) + \tau u(k) + \tau\tilde{f}(\eta(k), \xi(k))\end{aligned} \tag{6}$$

where $\eta \in \mathbb{R}^{n-m}$ and $\xi \in \mathbb{R}^m$. In this paper the results are applied to the single input case ($m = 1$). However the results can be easily extended to the multi-input case. Consider now the sliding surface parametrized by the gain $K \in \mathbb{R}^{m\times(n-m)}$ given by

$$s(k) = \xi(k) - K\eta(k) \tag{7}$$

such that,

$$\eta(k+1) = (I_{n-1\times n-1} + \tau A_{11} + \tau A_{12}K)\eta(k) + \tau A_{12}s(k) \tag{8}$$

obeys a predefined performance. Since the pair (A_{11}, A_{12}) is controllable, matrix K can be designed using any linear control design method in order to obtain practical stability. Then, the problem considered in this study focuses on designing the control action u such that the surface $s(k)$ is restricted in a QSM. Therefore, if the pair (η, s) is redefined as the state variables under study the following system is obtained ($\xi(k) = s(k) + K\eta(k)$)

$$\begin{aligned}\eta(k+1) &= \eta(k) + \tau(A_{11} + \tau A_{12}K)\eta(k) + \tau A_{12}s(k)\\ s(k+1) &= (K\eta(k) + s(k)) + \tau A_{21}\eta(k)\\ &\quad + \tau A_{22}(K\eta(k) + s(k)) + \tau u(k) + \tau\tilde{f}(\eta(k), \xi(k))\\ &\quad - K(\eta(k) + \tau(A_{11} + A_{12}K)\eta(k) + \tau A_{12}s(k))\end{aligned} \tag{9}$$

If the controller $u(k)$ satisfies the following structure

$$\begin{aligned}u(k) = &-(A_{21} + A_{22}K - KA_{11} - KA_{12}K)\eta(k)\\ &-(A_{22} - KA_{12})s(k) + v(k)\end{aligned} \tag{10}$$

then, the system (6) takes the form

$$\begin{aligned}\eta(k+1) &= \eta(k) + \tau(A_{11} + \tau A_{12}K)\eta(k) + \tau A_{12}s(k)\\ s(k+1) &= s(k) + \tau\tilde{f}(\eta(k), s(k) + K\eta(k), k) + \tau v(k)\end{aligned} \tag{11}$$

Now the problem considered in this research deals with designing the function $v(k)$ such that $s(k)$ becomes a QSM. This new form of the problem statement is solved with the application of a discrete version of the Super-Twisting algorithm (DSTA), which satisfies [15]:

$$\begin{aligned}v(k) &= -k_1\phi_1(s(k)) + w(k)\\ w(k+1) &= w(k) - \tau k_2\phi_2(s(k))\end{aligned} \tag{12}$$

where

$$\phi_1(s) = |s|^{1/2}\mathrm{sign}(s), \quad \phi_2(s) = \mathrm{sign}(s) \tag{13}$$

The correct selection of gains k_1 and k_2 makes possible to render the sliding surface into a QSM behavior.

Note that the uncertain function $\tilde{f}(\eta, s + K\eta, k)$ can be rewritten as

$$\begin{aligned}\tilde{f}(\eta, s + K\eta, k) &= g_1(\eta, s, k) + g_2(\eta, k)\\ g_1(\eta, s, k) &= \tilde{f}(\eta, s + K\eta, k) - \tilde{f}(\eta, K\eta, k)\\ g_2(\eta, k) &:= \tilde{f}(\eta, K\eta, k)\end{aligned} \tag{14}$$

Eq. (11) with the DSTA becomes

$$\begin{aligned}\eta(k+1) &= (I_{(n-m)\times(n-m)} + \tau A_{11} + A_{12}K)\eta(k) + A_{12}s(k)\\ s(k+1) &= s(k) - \tau(k_1\phi_1(s(k)) - w(k) + g_1(\eta, s, k))\\ w(k+1) &= w(k) - \tau(k_2\phi_2(s(k)) + dg_2(\eta, k))\end{aligned}$$

where $dg_2(\eta(k), k) = g_2(\eta(k+1), k+1)$. Let us introduce the following extended state vector $\theta := [\eta^{\top}\ s^{\top}\ w^{\top}]^{\top}$. This extended state vector satisfies the following recurrent dynamics

$$\theta(k+1) = \Phi(K)\theta(k) + B\mathrm{sign}(s(k)) + \Psi(k) \tag{15}$$

with

$$\Phi(K) = \begin{bmatrix}\Phi_{11} & A_{12} & 0\\ 0 & I_{m\times m} & \tau I_{m\times m}\\ 0 & 0 & I_{m\times m}\end{bmatrix}$$

$$\Phi_{11} = I_{(n-m)\times(n-m)} + \tau(A_{11} + A_{12}K)$$

$$B = \begin{bmatrix}0\\ -\tau k_1|s|^{1/2}\\ -\tau k_2\end{bmatrix}, \quad \Psi(k) = \begin{bmatrix}0\\ \tau g_1(\eta, s, k)\\ \tau dg_2(\eta, k)\end{bmatrix}$$

By assumption, the function $\tilde{f}(\eta, s + K\eta, k)$ is bounded, then

$$\|\Psi(k)\|^2 \le \varkappa_1\|\theta(k)\|_{\Lambda}^2 + \varkappa_2 \quad \forall k \ge 0 \tag{16}$$

where $\varkappa_1$ and $\varkappa_2$ are positive known constants and *Lambda* is a positive definite and symmetric matrix of appropriate dimensions. The main result of the paper is presented in the following theorem

Theorem 2. *Consider the nonlinear system given in (15), selecting* $k_1 > 0$ *and* $k_2 > 0$, *if the following matrix inequality*

$$\Phi^{\top}(K)(P + P(\Lambda_1 + \Lambda_2)P)\Phi(K) - (1 - \varrho)P + \varkappa_2\Lambda_2 < -Q \tag{17}$$

has a positive definite solution $P = P^{\top} > 0$ *then, the nonlinear dynamic system (15) is ultimately bounded with respect to* η *uniformly in* ξ *with bound*

$$\varepsilon := \frac{\left(\lambda_{\max}\{P\}\left(\xi_2^{+} + 2\frac{\gamma_0}{\varrho}\right) + \frac{\gamma_0}{\varrho}\right)}{\lambda_{\min}^{1/2}\{P\}} \tag{18}$$

where

$$\begin{aligned}&\gamma_0 := \delta_2 + \tfrac{1}{4}\delta_1^2\lambda_{\min}\left\{\overline{Q}^{-2}\right\}, \quad \delta_1 := \tau^4\omega k_1^2k_2^2 + z_{22}\tau^2k_1^2,\\ &\delta_2 := z_{33}\tau^2k_2^2 + 4z_{23}\omega^2 + \varkappa_2, \quad 0 \ge \varrho \ge 1,\\ &z_{i,j} = [\Lambda_1 + P]_{i,j\,=\,1:n-1}, \quad \Lambda_1 \in \mathbb{R}^{(n-1)\times(n-1)}, \quad \omega \in \mathbb{R}^{+}\end{aligned} \tag{19}$$

Proof. Consider the following Lyapunov candidate function given by

$$V(k) := \|\theta(k)\|_P^2$$

This function is bounded by two positive definite $\mathcal{K}$ functions as follows:

$$\lambda_{\min}\{P\}\|\theta(k)\|^2 \le \|\theta(k)\|_P^2 \le \lambda_{\max}\{P\}\|\theta(k)\|^2$$

If $\xi_2^{+} \in \mathbb{R}^{+}$ is the upper bound for the vector $\tilde{\theta} = [s \quad w]^{\top}$, the last equation turns in

$$\lambda_{\max}\{P\}\|\theta(k)\|^2 \le \xi_2^{+} + \|\eta(k)\|^2$$

Please cite this article as: Salgado I, et al. Control of discrete time systems based on recurrent Super-Twisting-like algorithm. ISA Transactions (2016), http://dx.doi.org/10.1016/j.isatra.2016.04.024

Then, both functions $\alpha(\cdot)$ and $\beta(\cdot)$ are defined as

$$\alpha(y)=\lambda_{\min}\{P\}y^2 \quad \beta(y)=\lambda_{\max}\{P\}\left(\xi_2^+ +2y^2\right)$$

Let $\Delta V(k)\coloneqq V(k+1)-V(k)$ then

$$\Delta V(k)=\theta^\top(k+1)P\theta(k+1)-\theta^\top(k)P\theta(k) \tag{20}$$

Substituting system (11) in (20) becomes

$$\Delta V(k)=\theta^\top(k)\left(\Phi^\top P\Phi-P\right)\theta(k)-2\theta^\top(k)\Phi^\top PB(k)\text{sign}(s(k)) +2\theta^\top(k)\Phi^\top P\Psi(k)+B(k)^\top PB(k)+\Psi^\top(k)P\Psi(k)$$

Using the following MI [21] $X^\top Y+Y^\top X\le X^\top\Lambda^{-1}X+Y^\top\Lambda Y$ $(X,Y\in\mathbb{R}^{n\times m},\ \Lambda=\Lambda^\top>0,\Lambda\in\mathbb{R}^{n\times n})$ and adding and subtracting $\varrho V(x)$, the last equation turns in

$$\Delta V(k)\le\theta^\top(k)\left(\Phi^\top\left(P+\Lambda_1^{-1}+\Lambda_2^{-1}\right)\Phi P\right)\theta(k)\theta(1-\varrho)\theta +B(k)^\top(P+\Lambda_1)B(k)+\Psi^\top(k)(P+\Lambda_2)\Psi(k)-\varrho V(x)$$

Expanding the term $B(k)^\top ZB(k)$ with $Z_1\coloneqq P+\Lambda_1$ and using the bounds described in (16)

$$B^\top(k)ZB(k)=z_{22}\tau^2k_1^2|s|+2z_{23}\tau^2k_1k_2|s|^{1/2}+z_{33}\tau^2k_2^2$$

Using again the matrix inequality mentioned above in the term that contains $|s|^{1/2}$ and considering the definition $Z_2=(P+\Lambda_2)$, and using the assumption that there exists a matrix $Q=Q^\top>0$ such that, MI given by (17) has a positive definite and symmetric solution P, then $\Delta V(k)$ becomes into (for any $\omega\in\mathbb{R}^+$)

$$\Delta V(k)\le-\theta^\top(k)Q\theta(k)+\delta_1|s|+\delta_2-\varrho V(k)$$

By Choleskii decomposition [21] with $\tilde{Q}=Q^{1/2}$ we obtain

$$\Delta V(k)\le-\left\|\overline{Q}\theta(k)\right\|^2+\delta_1\left\|\overline{Q}\ \overline{Q}^{-1}\theta(k)\right\|-\varrho V(k)+\delta_2$$

The arrangement of the terms in the previous inequality yields to

$$\Delta V(k)\le-\varrho V(k)+\delta_2+\tfrac{1}{4}\delta_1^2\left\|\overline{Q}^{-1}\right\|^2 -\left(\left\|\overline{Q}\theta(k)\right\|-\tfrac{1}{2}\delta_1\left\|\overline{Q}^{-1}\right\|\right)^T\left(\left\|\overline{Q}\theta(k)\right\|-\tfrac{1}{2}\delta_1\left\|\overline{Q}^{-1}\right\|\right)$$

Considering that the last term in the previous inequality is always negative

$$\Delta V(k)\le-\varrho V(k)+\delta_2+\tfrac{1}{4}\delta_1^2\lambda_{\min}\left\{(\overline{Q}^{-1})^2\right\} \tag{21}$$

Using the definition of γ_0 presented in Theorem 2, we can rewrite last equation as

$$\Delta V(k)\le-\varrho V(k)+\gamma_0\le-\varrho|x_1(k)|^2+\gamma_0$$

Defining the function γ as $\gamma(y)\coloneqq\varrho y^2$, $\Delta V(k)$ can be upper bounded by $\Delta V(k)\le-\gamma(|x_1|)+\gamma(\mu)$. Following the result given in Theorem 1 and Corollary 2, the bounds for the DSTA convergence are obtained as $\zeta=\beta(\mu)+\gamma(\mu)$ where $\mu^2\coloneqq\varrho^{-1}\gamma_0$. Therefore, using the previous definition, one has

$$\zeta(\mu)=\lambda_{\max}\{P\}\left(\xi^+ +2\mu^2\right)+\alpha\mu^2$$

and the upper bound for the equilibrium point of (15) is $(\varepsilon\triangleq\alpha^{-1}(\eta))$, that concludes the proof. □

The condition about the bound ξ_2^+ imposed on the vector $\theta=[s^\top\ w\top]^\top$ is a strong condition that sometimes cannot be accomplished in all the real cases. Therefore, to relax this condition the next corollary is introduced

Corollary 2. *If the MI in (17) is feasible for a positive definite solution $P=P^\top>0$, then, the equilibrium point of system (15) is ultimately bounded in a neighborhood around the origin with radius r defined as*

$$r=\frac{\gamma_0}{1-\varrho} \tag{22}$$

with γ_0 and ϱ defined in (19).

Proof. With the definition of γ_0 in (19), Eq. (21), is rewritten as

$$\Delta V(k)\le-\varrho V(k)+\gamma_0$$

And $\Delta V(k)=V(k+1)-V(k)$, then

$$V(k+1)\le(1-\varrho)V(k)+\gamma_0$$

The last equation is an invariant discrete time inequality and its solution can be obtained as

$$V(k+1)\le(1-\varrho)^kV(0)+\sum_{i=1}^{k}(1-\varrho)^{i-1}\gamma_0 \tag{23}$$

If the upper limit of last equation is taken, that is,

$$\overline{\lim_{k\to\infty}}(V(k))\le r \tag{24}$$

The Corollary 2 is proven. □

Remark 2. The solution of the MI showed in Eq. (17) seems to be a restrictive condition. However, this MI can be transformed into two LMIs. The MI in (17) is rewritten as

$$\Phi^\top(K)(P+P\tilde{\Lambda}P)\Phi(K)-(1-\rho)P+\varkappa\Lambda_2\le-Q \tag{25}$$

With $\tilde{\Lambda}=\Lambda_1^{-1}+\Lambda_2^{-1}$. If the next inequality is fulfilled

$$P+P\tilde{\Lambda}P\le G \tag{26}$$

that is equivalent (by Shur complement [21]) to

$$\begin{bmatrix}G-P & P\\ P & \tilde{\Lambda}^{-1}\end{bmatrix}\ge0 \tag{27}$$

The MI in (25) can be presented as

$$\Phi^\top(K)G\Phi(K)-(1-\rho)P+\varkappa I\le-Q \tag{28}$$

Then, the solution of (17) is relaxed to the solution of (27) and (28).

5. Numerical results

5.1. The stabilization problem

The DSTC is testing in a Furuta Pendulum, with dynamic model is given by the Euler–Lagrange formulation as

$$M(q)=\begin{bmatrix}M_{11}(q) & M_{12}(q)\\ M_{12}(q) & M_{22}(q)\end{bmatrix},\quad N(q,\dot{q})=\begin{bmatrix}N_1(q,\dot{q})\\ N_2(q,\dot{q})\end{bmatrix}$$

here

$$M_{11}(q)=J_{eq}+M_pr^2\cos^2(q_1)$$
$$M_{12}(q)=-\tfrac{1}{2}M_prl_p\cos(q_1)\cos(q_2)$$
$$M_{22}(q)=J_p+M_pl_p^2$$
$$N_1(q,\dot{q})=M_pr\left(-2r\cos(q_1)\sin(q_1)\dot{q}_1^2\right)+M_pr\left(\frac{1}{4}l_p\cos(q_1)\sin(q_2)\dot{q}_2^2\right)$$
$$N_2(q,\dot{q})=\tfrac{1}{2}M_pl_p\left(\sin(q_1)\cos(q_2)\dot{q}_1^2+g\sin(q_2)\right)$$

where $q=[q_1\ q_2]^\top$ are the generalized coordinates described in Fig. 1. q_1 is the angular rotation of the Furuta pendulum measured in the horizontal plane and q_2 is the angular rotation of the second arm that describes the Furuta pendulum, M_p is the mass of the pendulum, l_p is the length of pendulum center of mass from the

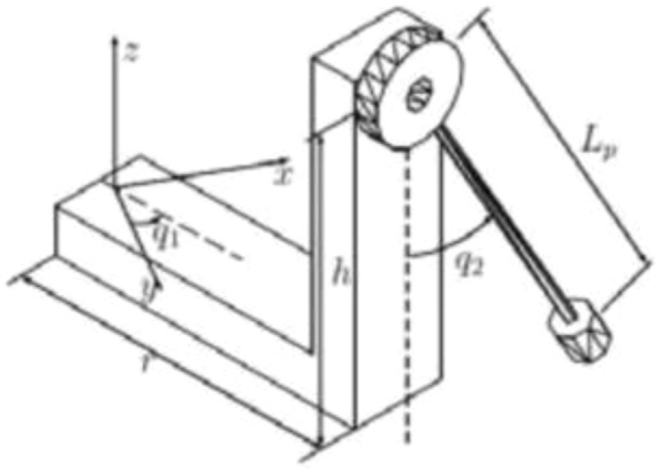

Fig. 1. Furuta pendulum and its generalized coordinates [22].

Table 1
Parameters of furuta pendulum.

Notation	Value	Units
M_p	0.027	kg
l_p	0.153	m
L_p	0.191	m
r	0.0826	m
g	9.810	m/s^2
J_{eq}	1.23×10^{-4}	kg m^2
J_p	1.10×10^{-4}	kg m^2

pivot, L_p is the total length of the pendulum, r is the length of the arm pivot to pendulum pivot, g is the gravitational acceleration constant, J_p is the pendulum moment of inertia about its pivot axis and J_{eq} is the equivalent moment of inertia about motor shaft pivot axis. The Physical parameters of the Furuta pendulum are defined in Table 1.

The equation of motion is linearized around $q^* = (\pi, 0) \in \mathbb{R}^2$. Thus, matrices A, B and C of the linear system are

$$A = \begin{bmatrix} 0 & 0 & 1 & 0 \\ 0 & 0 & 0 & 1 \\ -6.591 & 125.685 & -6.262 & 25.525 \\ 3.031 & -112.408 & 2.879 & -11.737 \end{bmatrix}$$

$$B = \begin{bmatrix} 0 \\ 0 \\ 56.389 \\ -25.930 \end{bmatrix}, \quad C = \begin{bmatrix} 0 \\ 1 \\ 0 \\ 0 \end{bmatrix}^\top \tag{29}$$

The gain K for the sliding surface (7) was obtained using the Ackerman–Utkin formula [1]. The DSTA with $k_1 = 10$ and $k_2 = 20$, was tested in the linearized system. The sampling period was settled as 0.01 s.

To obtain the bound ϵ we follow the next procedure: The matrix $\Phi(K)$ described in Eq. (15) is given by

$$\Phi(K) = \begin{bmatrix} 0.9989 & 0.0367 & 0 & 56.3890 & 0 \\ 0.0005 & 0.9831 & 0 & -25.9300 & 0 \\ -0.0001 & -3.0767 & 1.0000 & 4.3846 & 0 \\ 0 & 0 & 0 & 1.0000 & 0.0010 \\ 0 & 0 & 0 & 0 & 1.0000 \end{bmatrix}$$

Selecting $\varrho = 0.01$, $\varkappa_1 = 0.1$, $\varkappa_2 = 0.8$, $Q = 5 * I_{5\times5}$ and $\tilde{\Lambda} = \Lambda_1^{-1} + \Lambda_2^{-1} = I_{5\times5}$, the solution of (17) under the methodology proposed in Remark 2 is given by

$$P = \begin{bmatrix} 0.0352 & 0.0793 & 0.0175 & -0.0003 & -0.0000 \\ 0.0793 & 0.1861 & 0.0634 & 0.0258 & -0.0000 \\ 0.0175 & 0.0634 & 0.1447 & 0.0031 & 0.0000 \\ -0.0003 & 0.0258 & 0.0031 & 0.6750 & 0.0003 \\ -0.0000 & -0.0000 & 0.0000 & 0.0003 & 0.5348 \end{bmatrix}$$

and

$$G = \begin{bmatrix} 1.1945 & 0.1505 & 0.0336 & 0.0082 & -0.0000 \\ 0.1505 & 1.4775 & 0.1025 & 0.0624 & -0.0001 \\ 0.0336 & 0.1025 & 1.3021 & 0.0086 & 0.0000 \\ 0.0082 & 0.0624 & 0.0086 & 2.2485 & 0.0005 \\ -0.0000 & -0.0001 & 0.0000 & 0.0005 & 1.9640 \end{bmatrix}$$

The value of $\lambda_{\min}(\tilde{Q}^{-2}) = 1.4782$, from the solution P, the elements $z_{33} = 1.5348$ and $z_{23} = 0.003$ of matrix $Z = P + \Lambda_1$. Then from Corollary we obtain the values of $\gamma_0 = 0.8006$ and finally

$$r \leq \frac{0.8006}{1 - 0.01} = 0.8087 \tag{30}$$

This boundary condition can be easily verified in Figs. 2–5 where a comparison between three different control strategies is shown. The strategies used in simulation are a FOSM and a classical state feedback control. The gain applied in the FOSM was selected as $K_{FOSM} = 60$. And the control structure as

$$v = K_{FOSM} \text{sign}(s(k))$$

For the feedback controller, the Ackerman formula was employed to collocate the poles of the continuous Furuta pendulum described in Eq. (29) in $[-5\tau, -10\tau, 15-\tau, -20\tau]$. The gain obtained was injected in the signal control u as

$$u(k) = -K_{SF} x(k)$$

with $K_{SF} = [4.754, -18.8017, 0.0559, 32.001]$. Finally for the discrete controller based on the DSTA, the sliding surface was stabilized with a $K = [-19.5 \times 10^{-3}, 651.6 \times 10^{-3}, -3.99 \times 10^{-4}]$ obtained from the Ackerman formula collocating the poles in $[-1, -12-5]$. The gains for the DSTA were chosen as $k_1 = 60$, $k_2 = 30$. The coupled control perturbation for the simulation was selected as

$$\tilde{f}(k) = 0.1 \sin(10\tau k) - 0.5 \cos(5\tau k)$$

Finally, the sampling period was selected as 0.001 and the initial conditions were chosen as

$$x(0) = \begin{bmatrix} 2.5 & 0 & 0 & 0 \end{bmatrix}^\top \tag{31}$$

A total of 10,000 samples were simulated. In Fig. 2, the averaged trajectories for the pendulum position and the theta angle are shown. The control based on the DSTA shows a smooth behavior in contrast to the FOSM controller. This can be seen in the subfigure d, where the chattering phenomena appear. This classical disadvantage of FOSM was alleviated with discrete time high order sliding modes. Moreover, the zone of convergence is smaller when the DSTA is applied. In the case of the state feedback controller, with the previous parameters shows a faster convergence into a bigger zone than the other two controllers. Also, the overshot in the pendulum position is 10 times greater than the techniques involving discrete-time sliding mode theory.

In Fig. 3 the control signal is plotted. The energy used by the FOSM is bigger than the other controllers and presents fast oscillations. The feedback controller presents bigger overshoot but less oscillations. However, the convergence zone is bigger than the FOSM and DSTA. It seems that the DSTA presents better capabilities to control the Furuta pendulum, it offers less energy than the FOSM but better convergence than the state feedback

Please cite this article as: Salgado I, et al. Control of discrete time systems based on recurrent Super-Twisting-like algorithm. ISA Transactions (2016), http://dx.doi.org/10.1016/j.isatra.2016.04.024

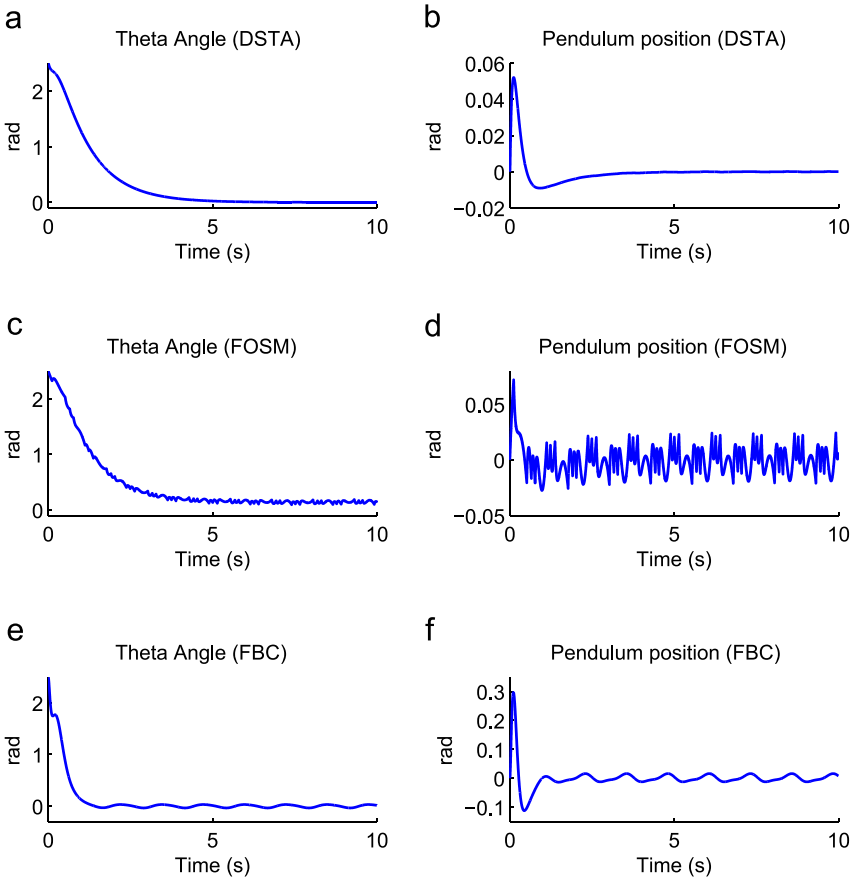

Fig. 2. Comparison between the DSTA, the FOSM and a state feedback controller (FB). The trajectories for the position and angle of a Furuta pendulum are obtained by simulations.

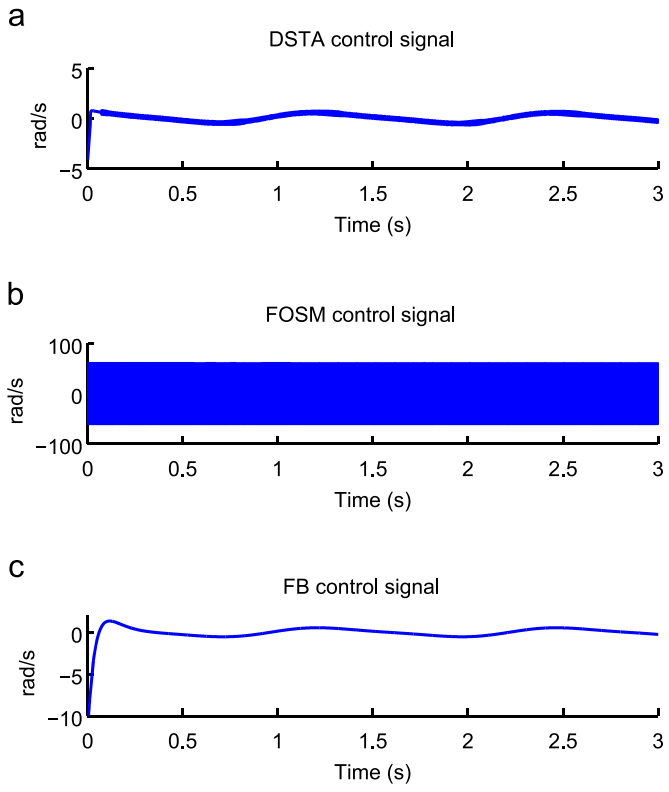

Fig. 3. Comparison between the control energy required for the DSTA, a first order sliding mode (FOSM) and a state feedback controller (FBC).

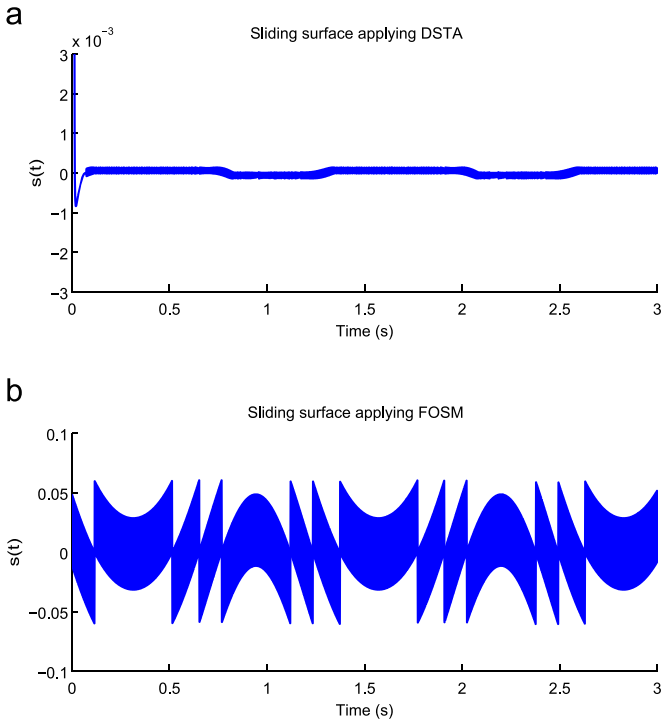

Fig. 4. Comparison between the sliding surface for a DSTA and a first order sliding mode (FOSM). The simulation time that is plotted was reduced to obtain a better appreciation of the signals.

Please cite this article as: Salgado I, et al. Control of discrete time systems based on recurrent Super-Twisting-like algorithm. ISA Transactions (2016), http://dx.doi.org/10.1016/j.isatra.2016.04.024

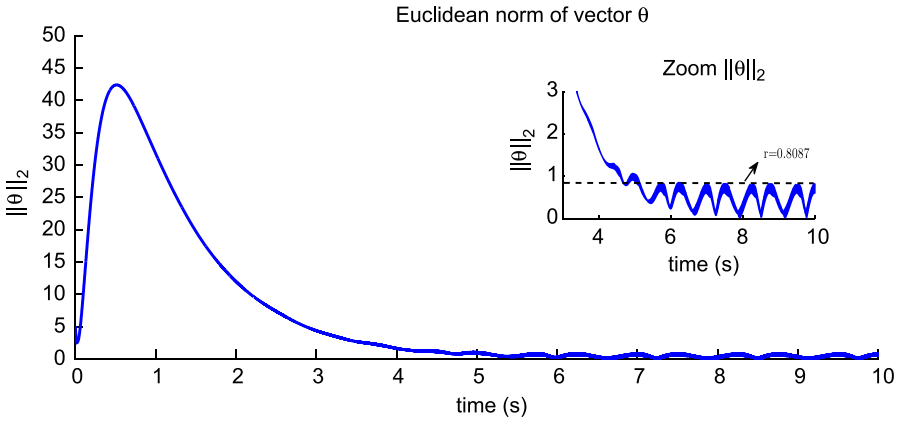

Fig. 5. Description of the boundary region defined by Eq. (30).

controller. In Fig. 4, the sliding surface for the FOSM and DSTA is shown. The QSM layer given by the DSTA is smaller than the FOSM. In Fig. 5 we can see the bound for the convergence of vector θ. This region of convergence coincides with the theoretical calculation provided by Corollary 2.

5.2. The differentiation and tracking problem

Consider the following lineal time invariant system equations that describe the dynamics for a DC-motor driver [19]

$$J\frac{d}{dt}\omega(t) = -b\omega(t)+k_t i(t)-T_L(t)$$
$$l\frac{d}{dt}i(t) = -k_e\omega(t)-ri(t)+v(t) \quad (32)$$

where $\omega(t)$ is the shaft speed, $i(t)$ is the motor current, $v(t)$ is the supply voltage, $T_L(t)$ is the load torque, J and b are the overall mechanical inertia and viscous friction coefficient at the motor shaft, respectively, k_t is the torque constant, l and r are the armature inductance and resistance, and k_e is the back electromagnetic-force constant. All motor parameters are assumed uncertain.

The shaft position Θ and the motor current i are available for measurement, while the shaft speed ω is assumed to be unknown. After an Euler discretization, the system described in (32) turns on

$$\omega(k+1) = \omega(k)+\tau J^{-1}[-b\omega(k)+k_t i(k)-T_L(k)]$$
$$i(k+1) = i(k)+\tau l^{-1}[-k_e\omega(k)-ri(k)+v(k)] \quad (33)$$

The structure for the closed loop for the complete discrete sliding mode control is depicted in Fig. 6.

As shown in Fig. 6 there exists an objective system, that is in the form of (33). The goal for the control action is to minimize the tracking error between the objective system and the real system shown in the block *DC-Drive*. If the error dynamics are defined according to Fig. 4. The equations in differences describing the error are

$$e_\omega(k+1) = e_\omega(k)+\tau\bar{J}^{-1}[-\bar{b}e_\omega(k)+\bar{k}_t i(k)-\bar{T}_L(k)]$$
$$e_i(k+1) = e_i(k)+\tau\bar{l}^{-1}[-\bar{k}_e e_\omega(k)-\bar{r}e_i(k)-v(k)+v^*(k)] \quad (34)$$

where $v^*(k)$ denotes a known control action applied to the objective system defined as $v^*(k) = 100\sin(k\tau)$ with τ being the sampled period and $v(k)$ is the action to be calculated under the DSTC technique. The terms with the upper bar represent a kind of uncertainties in the system parameters, that is, there exist some positive constants J^+, J^-, b^+, b^-, …, such that the following inequalities hold

$$J^- \le \bar{J} \le J^+ \quad b^- \le \bar{b} \le b^+ \quad k_t^- \le k_t \le k_t^+$$

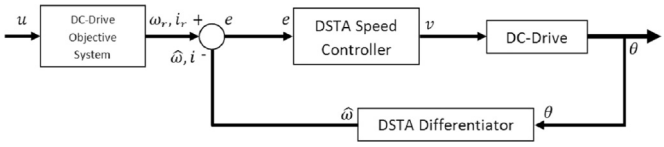

Fig. 6. Block scheme for the proposed controller using discrete STA as differentiator as well as controller.

Table 2
Parameters of DC motor system.

Notation	Value	Units
J	0.011	kg m^2
l	37×10^{-3}	μH
b	0.0005	N s
k_t	0.37	N A^{-1}
r	3.565	Ω
k_e	0.37	s rad^{-1}
v^*	$100\sin(k\tau)$	volts

$$l^- \le \bar{l} \le l^+ \quad r^- \le r \le r^+ \quad k_e^- \le k_e \le k_e^+$$

The error dynamics are already in the normal form described in (6), so it is straightforward to follow the procedure to use the proposed DSTA described in Eq. (12) and applied the final control action $v(k)$ in the form of (10).

The available output does not consider the angular velocity ω, so in the scheme depicted in Fig. 6, there is a block located in the feedback loop, that is a real discrete-time robust differentiator based on the DSTA, that provides a *finite-time-converging* estimation (in terms of the QSM concept described above) for the angular velocity $\hat{\omega}$.

The resulting differentiator based on the discrete super-twisting like algorithm as well as its proofs of convergence was presented in [15]. The parameters for the objective system are described in Table 2 [19].

It is assumed that the real system to be controlled has uncertainties. In the case of the second simulation, the parameters for the FOSM are $K_{FOSM} = 1000$. For the DSTA $k_1 = 500$ and $k_2 = 200$. The poles to stabilize the surface were selected as $[-2.91\ \ -3.91]$. Finally, the pole assignment for the state feedback controller was designed for the desired poles $[-1.91, -2.91, -3.1]$. The coupled perturbation was defined as $\tilde{f}(t) = 0.3\sin(20\tau k)-0.7\cos(10\tau k)$. The results obtained for this simulation are shown in Figs. 7–9. The sampling time τ was selected as 0.001.

Please cite this article as: Salgado I, et al. Control of discrete time systems based on recurrent Super-Twisting-like algorithm. ISA Transactions (2016), http://dx.doi.org/10.1016/j.isatra.2016.04.024

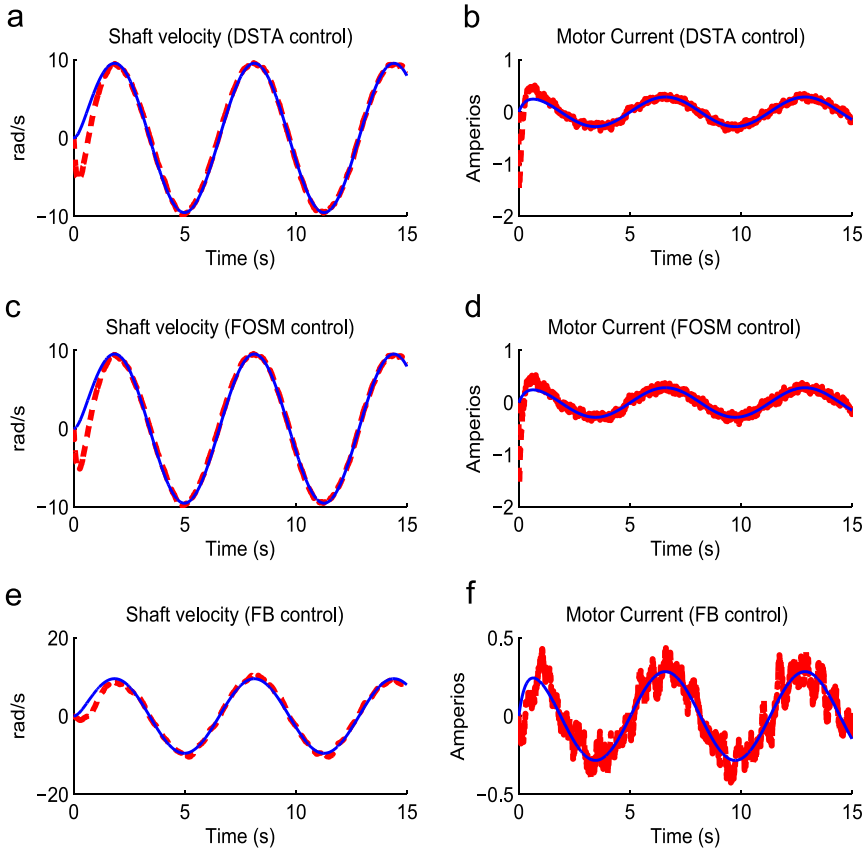

Fig. 7. Comparison between the DSTA, a first order sliding mode (FOSM) and a state feedback controller. The waveforms for the shaft velocity and the motor current plotted obtained by simulations. The blue line is the reference and the dotted red line represents the real waveforms. (For interpretation of the references to color in this figure caption, the reader is referred to the web version of this paper.)

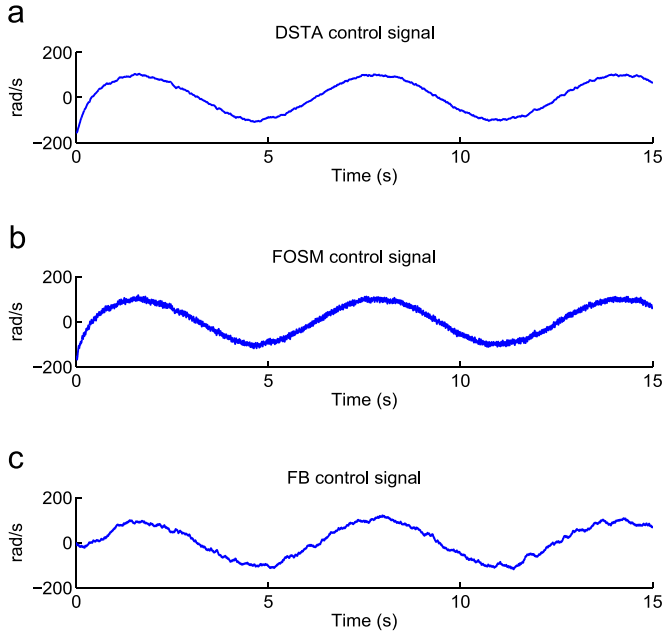

Fig. 8. Comparison between the three control signals: DSTA, a first order sliding mode (FOSM) and a state feedback controller.

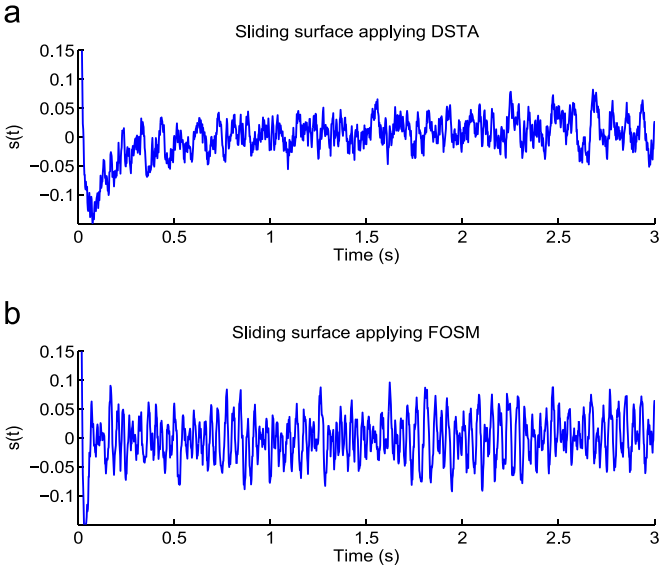

Fig. 9. Comparison between the sliding surface when the DSTA and a first order sliding mode (FOSM). The simulation time that is plotted was reduced to obtain a better appreciation of the signals.

In Fig. 7, the waveforms for the shaft velocity and motor current are plotted. It is possible to see with the state feedback controller how the real waveforms do not reach the reference as good as the techniques applying sliding modes. Also the oscillation in the motor current is bigger in the state feedback controller.

In Fig. 8, the control signals are depicted. The three controllers have a similar performance. However, the signal when the DSTA is applied is smooth and does not present the fast oscillations associated for a FOSM. We can see that the FOSM exhibits more oscillations than the control obtained by the DSTA. Taking into account that we are controlling a DC motor, these oscillations can damage this kind of electromechanical systems. In fact, this is the

Please cite this article as: Salgado I, et al. Control of discrete time systems based on recurrent Super-Twisting-like algorithm. ISA Transactions (2016), http://dx.doi.org/10.1016/j.isatra.2016.04.024

main disadvantage of FOSM theory. With the DSTA we can reduce these oscillations almost to a smooth signal. Finally, in Fig. 9, the behavior of the sliding surfaces is shown, the zone of convergence is reduced if the DSTA is implemented. The same procedure presented in the first numerical example can be followed in order to obtain the region of convergence r.

6. Conclusions

In this paper a Super twisting-like algorithm for discrete time systems has been presented. Finite time ultimate boundedness of the states was proved by means of the Lyapunov method for the control problem. Indeed, this is the main contribution proposed in this paper. Also, the upper bound of the neighborhood where the waveforms are converging is analytically calculated. The DSTA was applied as a controller (the pendulum example) and as a differentiator (control of a dc motor), preserving the characteristics that the Super-Twisting presents in the continuous time domain when a small sample period is chosen. The results obtained can be compared with the results obtained for the Super-Twisting control in continuous time. The discrete form for the controller can be implemented in a Microcontroller to be applied in other industrial applications.

Acknowledgment

Prof. Fridman and Prof. Bandyopadhyay would like to acknowledge the financial support provided by the Indo-Mexican project jointly funded by DST, India (DST/INT/MEX/RPO-02/08) and CONACYT, Mexico. Additionally Dr. Chairez wants to acknowledge the support provided by the CONACYT project numbered SEP-CB2013 221867.

References

[1] Utkin V. Sliding modes in control and optimization. Berlin: Springer-Verlag; 1992.
[2] Utkin V, Guldner J, Shi J. Sliding mode control in electro-mechanical systems. Autom. and control Eng. series. CRC Press; 2009 ISBN–13: 978-1420065602.
[3] Levant A. Sliding order and sliding accuracy in sliding mode control. Int J Control 1993;58(6):1247–63.
[4] Devant A. Principles of 2-sliding mode design. Automatica 2007;43(4):576–86.
[5] Drakunov SV, Utkin V. On discrete-time sliding mode. In: Proceedings of the IFAC symposium on nonlinear control systems design; 1989. p. 484–9.
[6] Miloslavjevic C. General conditions for the existence of a quasi-sliding mode on the sqitching hyperplane in discrete variable structure systems. Autom Remote Control 1985;46:679–84.
[7] Sira-Ramirez H. Nonlinear discrete variable structure systems in quasi-sliding mode. Int J Control 1991;54(5):1171–87.
[8] Bartoszewicz A. Discrete-time quasi-sliding mode control strategies. IEEE Trans Ind Electron 1998;45(4):633–7.
[9] Sarpturk SZ, Istefanopulos Y, Kaynak O. On the stability of discrete-time sliding mode control systems. IEEE Trans Autom Control 1987;32(10):930–2.
[10] Chang J-L. Robust discrete-time model reference sliding-mode controller design with state and disturbance estimation. IEEE Trans Ind Electron 2008;55:4065–74.
[11] Chakravarthini M, Bandyopadhyay B, Unbehauen H. A new algorithm for discrete-time sliding mode control using fast output sampling feedback. IEEE Trans Ind Electron 2002;49(2):518–23.
[12] Levant A. Finite differences in homogeneous discontinuous control. IEEE Trans Autom Control 2007;52(7):1208–17.
[13] Wang B, Yu X, Li X. Zoh discretization effect on higher-order sliding mode control systems. IEEE Trans Ind Electron 2008;55(11):4055–64.
[14] Davila J, Fridman L, Levant A. Second-order sliding-mode observer for mechanical systems. IEEE Trans Autom Control 2005;50(11):1785–9.
[15] Salgado I, Kamal S, Chairez I, Bandyopadhyay B, Fridman L. Super-twisting-like algorithm in discrete time nonlinear systems. In The 2011 International conference on advanced mechatronic systems, Zhengzhou, China, August, 2011.
[16] Bartolini G, Ferrara A, Usai E, Utkin V. On multi input chattering-free second-order sliding mode control. IEEE Trans Autom Control 2000;45(9):1711–9.
[17] Orlov Y, Aguilar L, Cadiou C. Switched chattering vonytol vs backlash/friction phenomena in electrical servo-motors. Int J Control 2003;76:959–67.
[18] Levant A, Fridman L. High order sliding modes. Sliding mode in control in engineering. New York, USA: Marcel Dekker, Inc.; 2002. p. 53–101.
[19] Pisano A, Davila A, Fridman L, Usai E. Cascade control of pm dc drives via second-order sliding-mode technique. IEEE Trans Ind Electron 2008;55 (11):3846–54.
[20] Haddad WM, Chellaboina V. Nonlinear dynamical systems and control. Princeton University Press; 2008.
[21] Poznyak A. Advanced mathematical tools for automatic control engineers. In: Deterministic systems, vol. 1. Elsevier Science; Hungary, 2008.
[22] Dávila A, Moreno J, Fridman L. Variable gains super-twisting algorithm: a Lyapunov based design. In: American control conference; 2010.

Please cite this article as: Salgado I, et al. Control of discrete time systems based on recurrent Super-Twisting-like algorithm. ISA Transactions (2016), http://dx.doi.org/10.1016/j.isatra.2016.04.024